Available online at www.sciencedirect.com
ScienceDirect
Scripta Materialia 59 (2008) 846–849
Scripta MATERIALIA
www.elsevier.com/locate/scriptamat

High strength and high ductility in a nanoscale superlattice of $Ni_2(Cr,Mo)$ deformable by twinning

H.M. Tawancy[a,*] and M.O. Aboelfotoh[b]

[a] *Center for Engineering Research, Research Institute, King Fahd University of Petroleum and Minerals, P.O. Box 1639, Dhahran 31261, Saudi Arabia*
[b] *Department of Materials Science and Engineering, North Carolina State University, Raleigh, NC 27695-7909, USA*

Received 3 June 2008; accepted 15 June 2008
Available online 25 June 2008

It is demonstrated that long-range ordering can be utilized to synthesize a nanoscale superlattice of $Ni_2(Cr,Mo)$ in a Ni–18.6 at.% Mo–15.1 at.% Cr. The superlattice is distinguished by high strength and high ductility. This behavior has been correlated with the crystallography of the disorder–order transformation, which favors deformation by twinning on the {1 1 1} planes of the parent face-centered cubic structure.
© 2008 Acta Materialia Inc. Published by Elsevier Ltd. All rights reserved.

Keywords: Aging; Nanocrystalline materials; Nickel alloys; Tension test; Transmission electron microscopy

Recently, there has been an increasing interest in developing nanoscale materials combining high strength and high ductility. Although several synthesis techniques have been advanced to produce such materials [1], modifications of various plastic deformation processes appear to be the most viable (e.g. [2–7]). These processes are based upon producing an ultra fine grain structure on the nanoscale by high plastic strain rate favoring deformation by twinning. In this paper, we demonstrate an alternative approach where long-range ordering in certain alloys can be utilized to synthesize nanoscale superlattices that combine high strength and high ductility. We have chosen a Ni–Cr–Mo alloy as a model system with an approximate composition of $Ni_2(Cr,Mo)$. Alloys based upon this system have many important high- and low-temperature applications in the petrochemical, chemical process, and power generation industries. Similar to the case of the Ni–Mo system, these alloys are known to undergo a series of long-range ordering reactions resulting in the formation of the closely-related DO_{22} (Ni_3Mo), $D1_a$ (Ni_4Mo), and Pt_2Mo-type superlattices [8]. Although these superlattices can co-exist during the early stages of ordering, it has been shown that the most stable ordered phase which forms in a given alloy is a sensitive function of chemical composition [8–11].

The alloy studied here had a composition of Ni–26.97 wt.% Mo–11.95 wt.% Cr corresponding to Ni–18.5 at.% Mo–15.1 at.% Cr. Bulk samples were processed into sheets about 1.5 mm in thickness, and then annealed at 1065 °C for 15 min followed by water quenching. Long-range ordering was induced by thermal aging at 700 °C. Transmission electron microscopy (TEM) and diffraction as well as high-resolution transmission electron microscopy (HRTEM) were used to characterize the microstructure. Thin-foil specimens were prepared by the jet polishing technique. Mechanical strength was determined from room-temperature tensile tests carried out on standard samples with 50.8 mm gage length. All crystallographic notations are given in terms of the parent face-centered cubic (fcc) structure of the ordered phases.

As shown in Figure 1a–c, the DO_{22}, D1a, and Pt_2Mo-type superlattices can directly be derived from the parent fcc lattice by minor atomic rearrangement on the {4 2 0} planes as shown in Figure 1a–c. Figure 1d shows a schematic of the (001) reciprocal lattice intersection illustrating the relative positions of the corresponding superlattice reflections. As can be seen, the characteristic reflections of the DO_{22} superlattice are located at ⟨1 1/2 0⟩, ⟨100⟩, and ⟨1 1 0⟩ positions, and those of the $D1_a$ and Pt_2Mo-type superlattices are located at 1/5 ⟨420⟩ and 1/3 ⟨420 (or equivalently 1/3 ⟨220⟩), respectively. Although Ni_2Mo is not thermodynamically stable in the Ni–Mo system, it can stabilized by additions of Cr since Ni_2Cr is stable in the Ni–Cr system.

* Corresponding author. Tel.: +966 3 860 4317; e-mail: tawancy@kfupm.edu.sa

1359-6462/$ - see front matter © 2008 Acta Materialia Inc. Published by Elsevier Ltd. All rights reserved.
doi:10.1016/j.scriptamat.2008.06.026

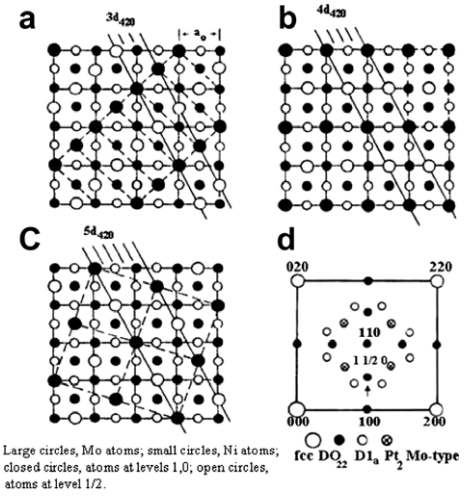

Figure 1. Schematics illustrating the atomic arrangements of various superlattices along ⟨0 0 1⟩ direction and relative positions of respective superlattice reflections: (a) DO_{22} superlattice, (b) $D1_a$ superlattice, (c) Pt_2Mo-type superlattice, (d) ⟨0 0 1⟩ reciprocal lattice intersection.

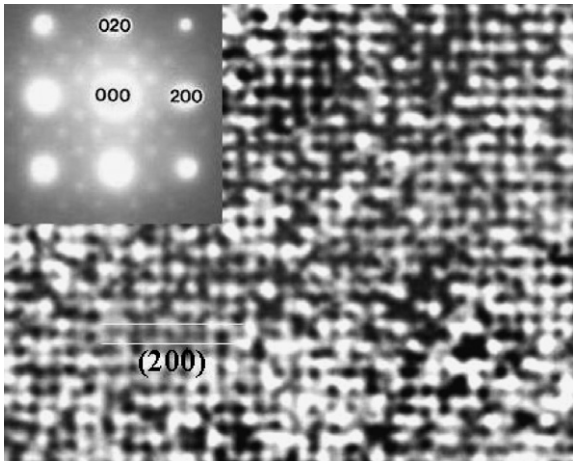

Figure 2. State of short-range order in the as-quenched condition illustrated by ⟨0 0 1⟩ diffraction pattern and corresponding HRTEM image.

In the as-quenched condition, diffuse intensity maxima due to short-range order were observed at ⟨1 1/2 0⟩ positions similar to the case of Ni–Mo alloys [8–13]. Also, the corresponding HRTEM images resembled those obtained in the case of Ni4Mo as shown in the example of Figure 2. Using multi-slice image simulations, an image such as that shown in Figure 2 has been interpreted in terms of subunit cell clusters of the DO_{22}, $D1_a$, and Pt_2Mo-type superlattices using multi-slice image simulations [14]. A further evidence for the co-existence of these superlattices in the present case is provided by electron diffraction as shown below.

Figure 3 illustrates the ⟨0 0 1⟩ electron diffraction pattern as a function of thermal aging time at 700 °C. As shown earlier, diffuse intensity maxima are observed at {1 1/2 0} positions in the annealed state (Figure 3a). During the early stages of thermal exposure (5 min at 700 °C), those intensity maxima became elongated along ⟨1 0 0⟩ directions suggesting the onset of formation of DO_{22} superlattice (Fig. 3b). With continued exposure, characteristic reflections of the three superalattices be-

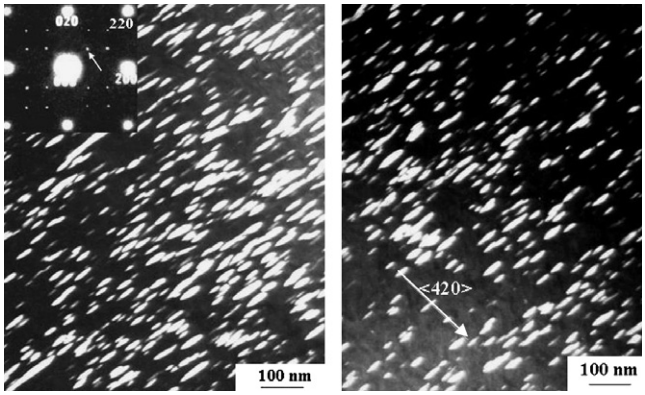

Figure 4. Dark-field TEM images formed with 1/3⟨2 2 0⟩ superlattice reflections to illustrate the morphology of ordered particles as a function of aging time at 700 °C: (a) 24 h; the inset is a ⟨0 0 1⟩ diffraction pattern, (b) 100 h.

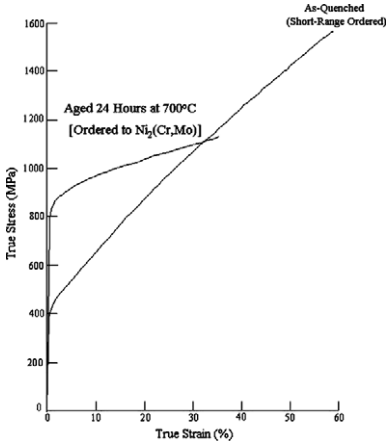

Figure 5. Comparative true stress–strain diagrams in the disordered and ordered states.

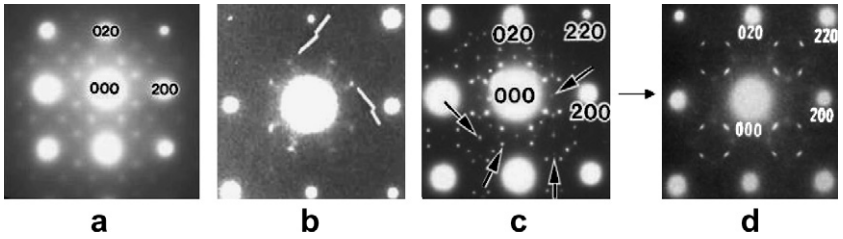

Figure 3. ⟨0 0 1⟩ selected-area diffraction patterns illustrating the transition from short-range order into long-range order during thermal aging at 700 °C: (a) as-quenched, (b) 5 min at 700 °C, (c) 15 min at 700 °C, (d) 8 h at 700 °C.

Download English Version:

https://daneshyari.com/en/article/1501731

Download Persian Version:

https://daneshyari.com/article/1501731

Daneshyari.com